

# Effect of microstructure on low cycle fatigue behavior of Inconel 706 at 650 °C

Sangshik Kim<sup>1</sup>, Kwangyeon Kim<sup>1</sup>, Junmin Lee<sup>1</sup>, and Jung Gi Kim<sup>1</sup>

<sup>1</sup>Gyeongsang National University College of Engineering

July 11, 2023

## Abstract

Four different types of specimens were prepared from the center and the periphery of two large IN706 forged discs of commercial scale, and low cycle fatigue (LCF) tests were conducted at 650 °C. The IN706 specimens with lower LCF lives showed relatively large fraction of cleavage-like fracture along linearly aligned  $\eta$  ( $\text{Ni}_3\text{Ti}$ ) precipitates in the area of crack propagation. The amount of  $\eta$  precipitates for those specimens with greater LCF lives was negligible, and the fracture mode of crack propagation was dominantly intergranular. Crack initiation was mainly by persistent slip band (PSB) cracking at the surface, and no notable difference was found for each specimen. The correlation between tensile properties, grain size and LCF lives of IN706 at 650 °C appeared to be not as significant as expected.

## Hosted file

Manuscript.docx available at <https://authorea.com/users/638191/articles/654068-effect-of-microstructure-on-low-cycle-fatigue-behavior-of-inconel-706-at-650-o-c>

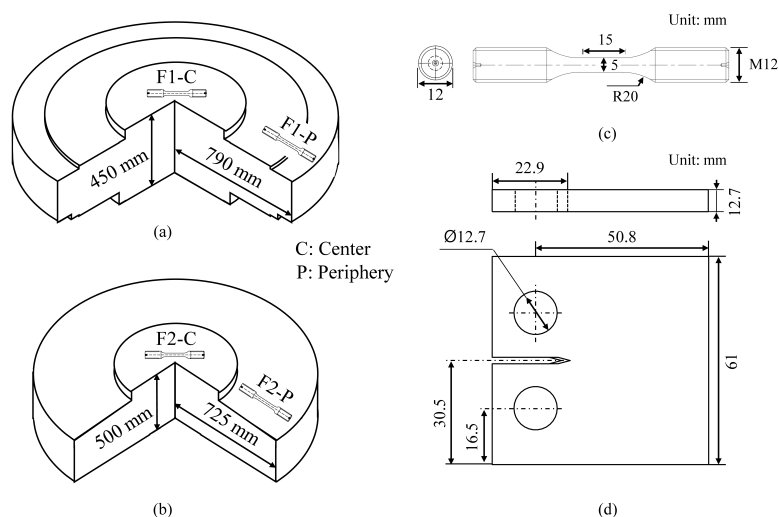


Fig. 1 - The schematic illustration of forged discs of IN706, (a) F1 and (b) F2, along with the location of specimen preparation and the schematic diagram showing (c) hour glass type specimen for LCF test and (d) CT specimen for FCP test.

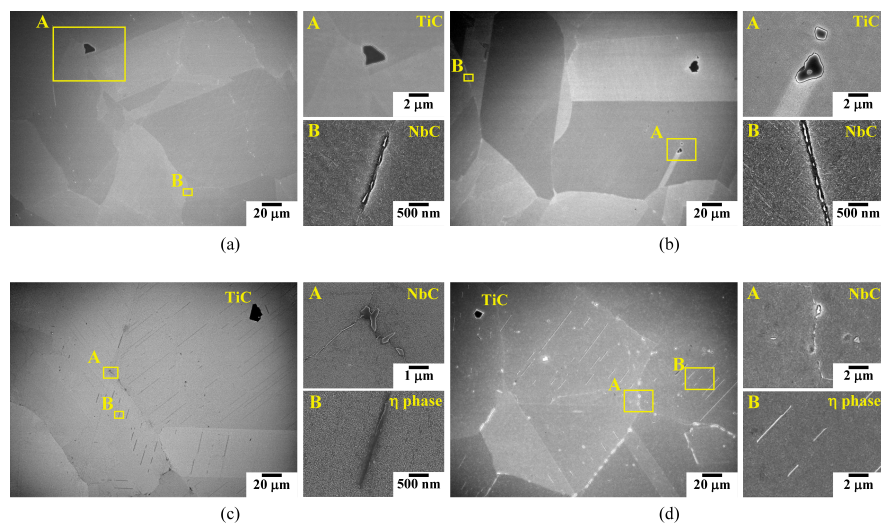


Fig. 2 - The SEM micrographs of (a) F1-C, (b) F1-P, (c) F2-C and (d) F2-P specimens prepared from various locations of forged IN706 discs.

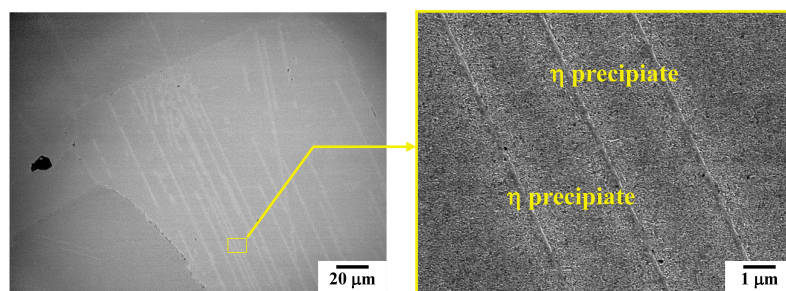


Fig. 3 - Linearly aligned  $\eta$  ( $\text{Ni}_3\text{Ti}$ ) precipitates in F2 specimen.



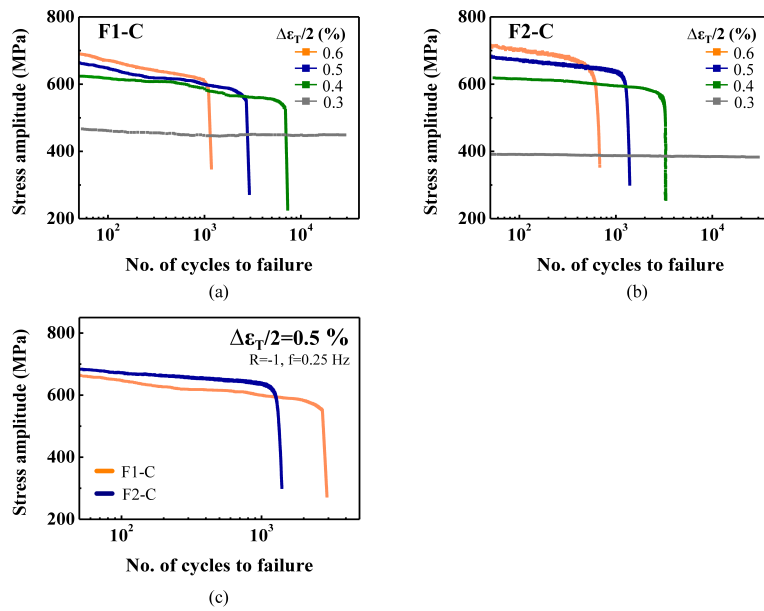


Fig. 4 - The stress amplitudes of (a) F1-C specimens and (b) F2-C specimens as a function of number of cycles at different strain amplitude of 0.6, 0.5, 0.4 and 0.3 %, respectively, and (c) those of F1-C and F2-C specimens at a strain amplitude of 0.5 %.

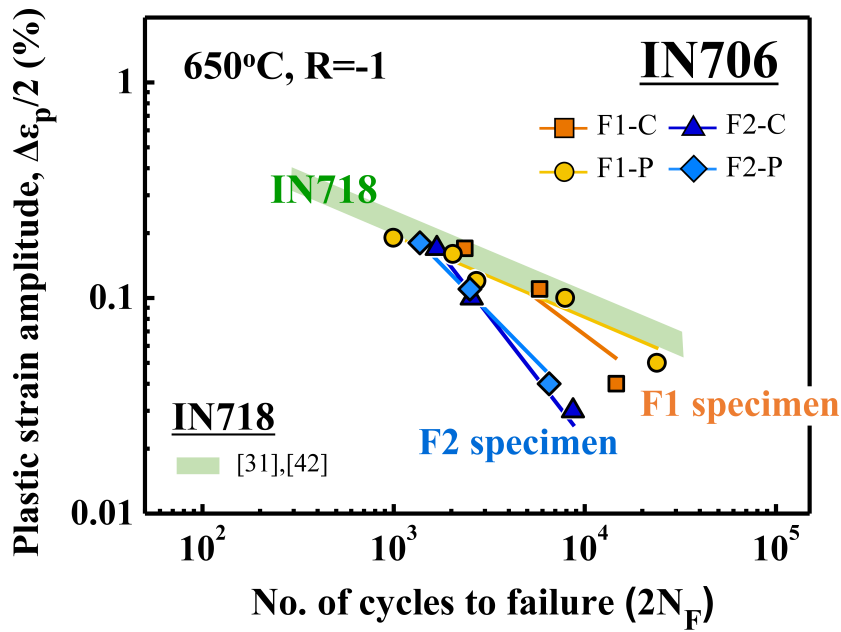


Fig. 5 - The Coffin-Manson plots of F1-C, F1-P, F2-C and F2-P specimens at 650°C.

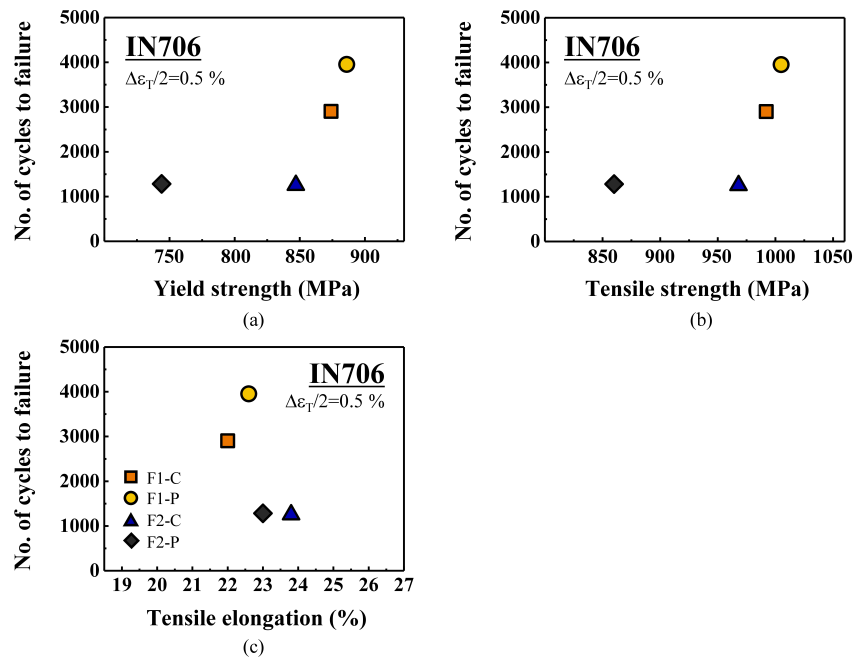


Fig. 6 - The number of cycles for F1 and F2 specimens at an applied total strain of 0.5 % as a function of (a) yield strength, (b) tensile strength and (c) tensile elongation at 650°C.

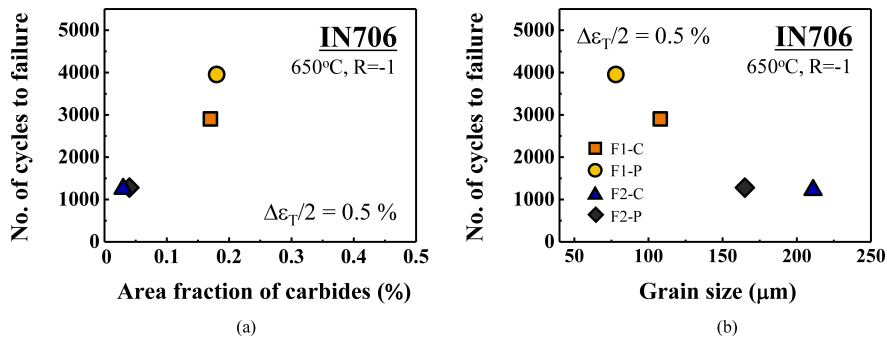


Fig. 7 - The number of cycles to failure for F1 and F2 specimens at an applied total strain of 0.5 % as a function of (a) the area fraction of carbides and (b) the size of grain.

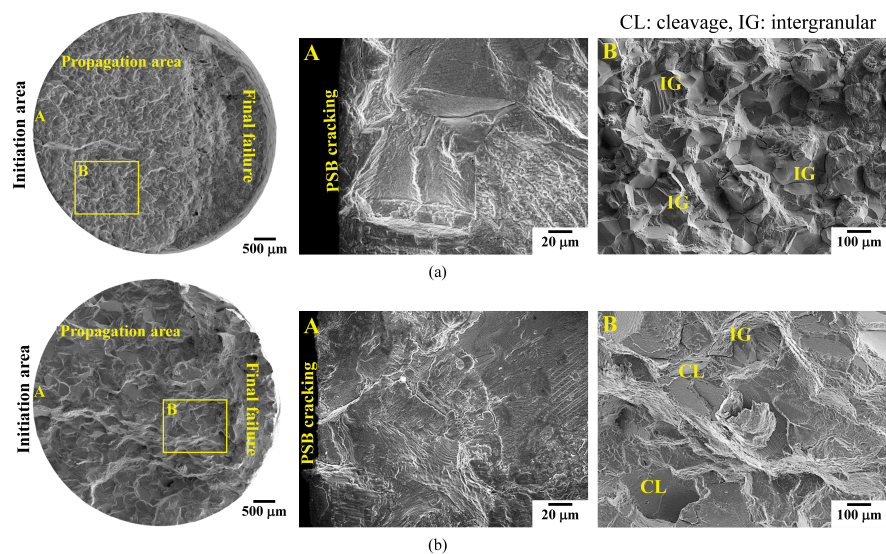


Fig. 8 - Low magnification SEM fractographs of (a) F1-C and (b) F2-C specimens, and high magnification fractographs showing the area of initiation (A) and propagation (B).

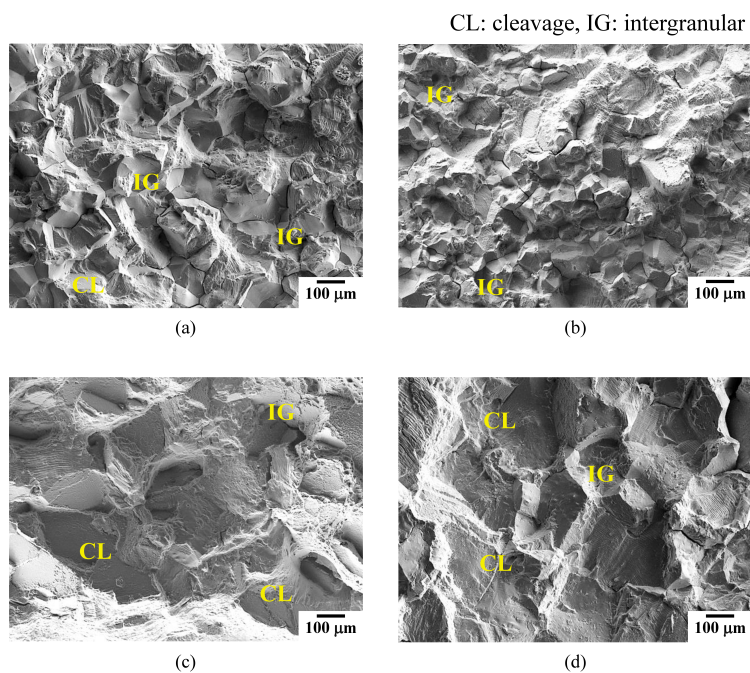


Fig. 9 - The SEM fractographs of (a) F1-C, (b) F1-P, (c) F2-C and (d) F2-P specimens, documented in the area of propagation.

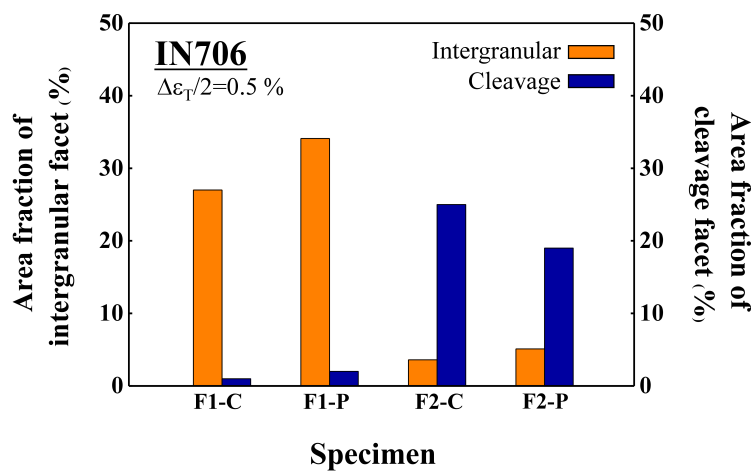


Fig. 10 - The area fraction of cleavage facet and intergranular facet in LCF-tested IN706 specimen.

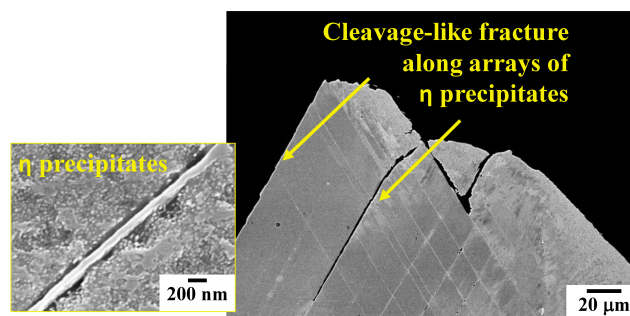


Fig. 11 - The cross sectional view of cleavage like fracture along arrays of  $\eta$  precipitates in F2-C specimen.

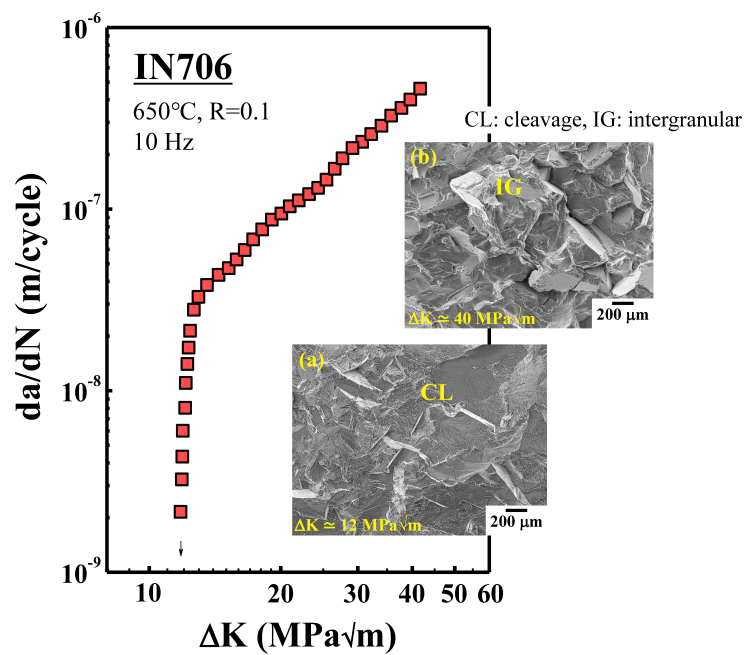


Fig. 12 - The  $da/dN$  vs  $\Delta K$  curve of IN706 alloy at 650°C and the SEM fractographs at  $\Delta K$  value of (a) 12 and (b) 40  $\text{MPa}\sqrt{\text{m}}$ , respectively.

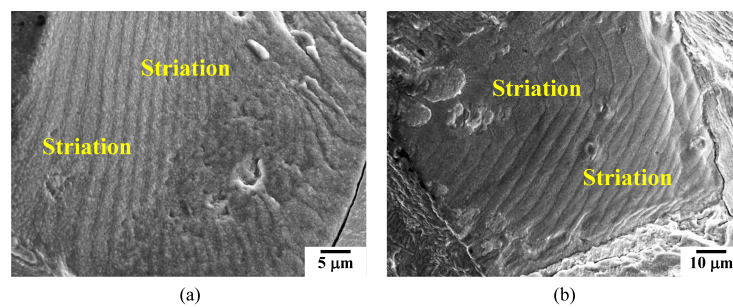


Fig. 13 - The SEM fractographs showing striations on LCF-tested (a) F1-C and (b) F2-C specimen, documented in the area of propagation.